Gliosarcoma: Neuroimaging and Immunohistochemical Findings

Miriam E. Peckham, Anne G. Osborn, Cheryl A. Palmer, Amy Tsai, Karen L. Salzman

From the Department of Radiology and Imaging Sciences, University of Utah Health Sciences Center, Salt Lake City, UT (MEP, AGO, AT, KLS); and Department of Pathology, University of Utah Health Sciences Center, Salt Lake City, UT (CAP).

ABSTRACT

BACKGROUND AND PURPOSE: Gliosarcoma (GSC) is an intra-axial lesion which often abuts a dural margin and is composed of glial and mesenchymal elements. This lesion is considered a variant of isocitrate dehydrogenase (IDH)-wild type glioblastoma (GBM). The purpose of this study is to evaluate the imaging and molecular features of GSC in a large patient cohort.

METHODS: Pathology-proved GSC cases were collected from our quaternary care center spanning the last 16 years and IDH status was documented. Older GSC cases without prior immunohistochemical testing underwent tissue block staining to obtain IDH status. When available, p53, phosphate and tensin (PTEN), MIB-1, EGFR amplification, and MGMT methylation were recorded and imaging findings tabulated. Logistic regression analyses were performed to determine correlation of molecular markers and imaging characteristics.

RESULTS: A total of 25 cases were identified (21 de novo, 4 post-treatment). All lesions contacted a dural, pial, or ependymal surface and were negative for an IDH R132H mutation, including postradiation GSC. In total, 16 of 16 cases showed nonamplification of EGFR/CEP7, 2 of 16 demonstrated MGMT methylation, and multiple lesions demonstrated p53 and PTEN mutations. Imaging features included areas of nodular thickening in necrotic lesions which appeared to abut the site of dural contact. There was no significant correlation of molecular markers with imaging characteristics.

CONCLUSION: GSC was IDH(−) in all cases, supporting the current understanding of this lesion being a wild-type GBM variant. Additional molecular markers demonstrated no significant correlation with imaging findings in this cohort.

Keywords: Gliosarcoma, oncology, immunostaining, MRI.

Acceptance: Received July 22, 2018, and in revised form September 17, 2018. Accepted for publication September 18, 2018.

Correspondence: Address correspondence to Miriam E. Peckham, MD, Department of Radiology and Imaging Sciences, University of Utah Health Sciences Center, 30 North, 1900 East #1A071, Salt Lake City, UT 84132-2140, USA. E-mail: Miriam.Peckham@hsc.utah.edu.

Acknowledgments and Disclosure: No funding was provided for this research. The authors declare that there is no conflict of interest regarding the publication of this paper.

J Neuroimaging 2019;29:126-132.
DOI: 10.1111/jon.12565

Introduction

The 2016, the World Health Organizations' Classification of Tumors of the Central Nervous System redrew the family trees of diffuse gliomas, classifying according to their molecular characteristics, one of which is isocitrate dehydrogenase (IDH) status.[1–3] The IDH profile of glioblastoma (GBM) and other high-grade glial tumors has been well established in large case studies.[4] The IDH profile of the more rare gliosarcoma (GSC), a grade IV lesion comprising approximately 2% of all GBM, has been studied in multiple nonimaging series.[5–7]

In the largest known histologic study of 36 patients, GSC was found to be universally IDH wild-type, suggesting that it is a derivative, or genetic variant of primary GBM.[5] However, IDH-mutated GSC has been reported, with 2 of 26 cases in a prior study demonstrating the presence of IDH1 mutation. No IDH2 mutation has been reported.[8]

Typical imaging characteristics of GSC are that of a supratentorial intracranial lesion which most often abuts a dural surface, is peripherally located, and demonstrates irregular rim enhancement.[7,9–13] Though multiple imaging-based case series of varying sizes have been reported, correlative IDH immunostaining has not been incorporated. We present the largest known radiologic case series with immunohistochemical and histologic correlation and delineate their imaging spectrum.

Methods

Institutional Review Board approval was obtained in this retrospective study and informed consent was waived. All investigators complied with the Health Insurance Portability and Accountability Act and Good Clinical Practice guidelines.

A report search was performed for cases of GSC in our quaternary care center spanning the last 16 years. All histopathologic specimens were reviewed by a neuropathologist to confirm the original diagnosis of GSC and, when available, IDH1, Epidermal Growth Factor/centromere enumerating probe 7 (EGFR/CEP7), and O6-methylguanine-DNA methyltransferase (MGMT) status were recorded. In cases where IDH staining had not initially been performed, IDH R132 staining was performed on available tissue blocks. Evaluation for rarer IDH1/2 mutations was not performed.

MR imaging characteristics were evaluated by a neuroradiology attending with greater than 30 years' experience and a neuroradiology fellow. Characteristics were recorded in each case with special attention to the following sequences: Fluid attenuated inversion recovery (FLAIR), postcontrast T1, and T2*/susceptibility weighted imaging (SWI)/gradient echo (GRE). Additional sequences were reviewed as available. In each case, lesion location, size, T2/FLAIR characteristics, enhancement pattern (categorized as peripheral in cases with a

Table 1. Subject Demographics

Total subjects	25
Age at diagnosis	62 +/– 16.4 y
Sex	12 F/13 M
Survival (months)	11.8
De novo	21
Treatment-induced	4
IDH-wild type	25/25
EGFR/CEP7	16/16 nonamplified
MGMT	2/16 detected

Demographic information.
Y = years; F = female; M = male.

prominent nonenhancing necrotic core, diffuse when there was near complete enhancement involving >90% of the lesion, and mixed for lesions demonstrating both peripheral and partial internal enhancement), and lesion composition (whether predominantly solid or necrotic) were recorded. The presence of extracranial extension was also noted. The presence of hemorrhage and restriction on GRE and diffusion weighted imaging (DWI) findings were recorded. The amount and presence of restriction on DWI, and hemorrhage on GRE, involving the solid portions of the lesions was determined qualitatively by visual assessment with cases categorized as demonstrating no signal abnormality, trace signal abnormality, <50%, and >50% abnormality.

Demographic and clinical information was obtained on all patients. This included patient age and sex, presenting symptoms, type of therapy, and overall survival time.

Statistical Analysis

Logistic regression analysis was performed to determine correlation of molecular markers with the following: overall survival, tumor size, enhancement characteristics, lesion nodularity at the site of dural attachment, extracranial extension, and tumor composition. Correlation was performed between survival time and percent sarcomatous components of the lesions. Analyses were performed using Stata 14 (Stata Statistical Software: Release 14; College Station, TX, USA).

Results

A report search revealed 31 cases of pathology-proven GSC. Twenty-seven of these cases had available preoperative MR imaging. Of these cases, 17 had IDH-staining, while 10 cases lacked IDH immunostaining as they were evaluated before the time when IDH staining was in clinical use. Tissue blocks were available in 8 of these 10 subjects and IDH staining was performed at the time of the study. This resulted in a total of 25 cases with both MR imaging and IDH staining in 12 female and 13 male patients ranging in age from 5 to 87 years (average age of 62.0 +/– 16.4 years, Table 1). Twenty-one of these cases were diagnosed as de novo GSC and 4 cases arose within the resection cavity of a treated glioma (1 from a grade 2 diffuse fibrillary astrocytoma, 1 from a grade 3 anaplastic ependymoma, and 2 from GBM). Three cases arose within 2 years of original resection (8, 9, and 19 months), and the fourth lesion arose 26 months after resection. Three of these four patients had documented history of radiation, with no records available for the fourth patient. One patient had GSC diagnosed within 3.5 months of radiation therapy (total of 6,000 cGy) and one patient had recurrence within 6 months of radiation therapy (total of 5,940 cGy). The third patient had recurrence within 16 months but dose was not specified.

Histopathologic and Immunohistochemical Characteristics

Histologically, all lesions demonstrated a mixture of glial and sarcomatous components. In 23 of 25 cases, a determination of percent sarcomatous components could be rendered by a pathologist, with 13 of 23 lesions demonstrating predominantly glial components (50% or greater), and the remainder demonstrating predominantly sarcomatous components.

All cases were negative for an IDH R132 mutation. All cases had nonamplification of EGFR/CEP7 by fluorescence in-situ hybridization techniques. MGMT status by a polymerase-chain reaction was also performed in 16 cases and methylation was detected in 2. P53 immunostaining was obtained in 16 subjects and, and using a cutoff of 30%, was positive in 13. Phosphate and tensin (PTEN) immunostaining was obtained in 14 subjects and was positive in 9 using a cutoff of 50%. Methylation-inhibited binding protein 1 (MIB-1) immunostaining was obtained in 17 subjects and was greater than 20% in all (Table 2).

Imaging Characteristics

The most common tumor location was the temporal lobe, seen in 13 of 25 subjects. The frontal lobe was the second most common site (10 of 25 subjects), and parietal and occipital lobes the least common sites (2 of 25 subjects). Right-sided lesions predominated, seen in 17 of 25 subjects. Lesion size ranged from 2.3 to 7.5 cm (mean of 5.6 cm) in greatest dimension.

All subjects had T1 and T1-post contrast imaging, and 24 of 25 had T2-weighted imaging. All but one subject had DWI, and 22 of 25 subjects had susceptibility (T2*/SWI/GRE) imaging. All de novo tumors contacted a surface whether dural, ependymal, or surface along the brain parenchyma (presumed pial), with 17 lesions contacting the dura mater, 3 lesions contacting the ependymal surfaces, and 1 lesion contacting a pial surface. All treatment-induced tumors also showed pial or dural contact (3 of 4 dural, 1 of 4 pial). One case showed no dural contact when it originally presented as a high-grade GBM, but was found to contact a dural surface after GSC arose in the treatment cavity. All tumors enhanced, with the majority demonstrating mixed or diffuse enhancement without significant necrotic regions (10 mixed and 5 diffuse), and the remaining 10 demonstrating predominantly peripheral enhancement, most in the setting of a necrotic core.

Additional imaging characteristics included a predominantly centrally necrotic or mixed appearance in approximately half of de novo lesions (13 of 21), with all but one of the necrotic tumors demonstrating nodular, enhancing mass-like thickening (T1/T2 isointense) abutting the site of pial or dural attachment (Fig 1). The remaining de novo tumors were predominantly solid with darker T2 signal characteristics and diffuse enhancement with no significant necrosis. Susceptibility imaging had variable findings demonstrating trace to <50% of hemorrhagic products in the majority of subjects who had a GRE sequence (12 of 22). When present, hemorrhagic products predominated within the nodular mass-like component of the more necrotic lesions. Diffusion imaging was variable, with 11 subjects showing no restriction and the remaining subjects

Table 2. Clinical and Molecular Characteristics of GSC

Case	Age	Sex	De Novo	Therapy	Survival (m)	IDH	EGFR/CEP7	MGMT	p53 (>30%)	PTEN	MIB-1 (>20%)	Sarcoma Component (%)
1	76	F	y	S	3.5	–	–	–	+	–	+	20
2	72	M	y	S/XRT/C	Unk	–	–	–	+	+	+	10
3	77	M	y	S/XRT/C	10	–	–	–	+	+	+	50
4	47	M	y	S	16	–	–	–	+	+	+	50
5	77	M	y	S/XRT/C	15	–	–	–	+	+	+	10
6	74	M	y	S/XRT/C	9.5	–	–	–	+	–	+	20
7	58	M	y	S/XRT	18.5	–	–	–	–	–	+	80
8	72	F	y	S/XRT	Unk	–	–	–	–	+	+	15
9	58	M	y	S/XRT/C	Unk	–	–	–	+	–	+	10
10	70	M	y	S/XRT/C	11	–	–	–	+	+	+	50
11	65	M	y	S/XRT	13	–	–	+	+	+	+	30
12	64	F	y	Unk	1.5	–	–	+	Unk	Unk	Unk	10
13	53	F	y	S/XRT/C	Unk	–	–	–	+	–	+	60
14	51	F	n	S/XRT/C	Unk	–	–	Unk	Unk	Unk	Unk	60
15	43	F	y	S/XRT/C	Unk	–	–	–	+	+	+	50
16	53	F	n	None	6	–	Unk	Unk	–	+	+	NE
17	74	F	y	S/XRT/C	Unk	–	-	–	+	+	+	70
18	67	F	y	Unk	Unk	–	Unk	–	+	+	+	NE
19	5	F	y	Unk	Unk	–	Unk	Unk	Unk	Unk	Unk	20
20	59	F	n	Unk	3	–	Unk	Unk	Unk	Unk	+	70
21	51	M	n	S/XRT/C	5	–	Unk	Unk	Unk	Unk	Unk	60
22	87	F	y	S/XRT	4	–	Unk	Unk	Unk	Unk	Unk	20
23	74	M	y	S	.5	–	Unk	Unk	Unk	Unk	Unk	25
24	52	M	y	S/XRT/C	66	–	Unk	Unk	Unk	Unk	+	30
25	70	M	y	S/XRT/C	7	–	Unk	Unk	Unk	Unk	Unk	20

All subjects with corresponding clinical, immunostaining, and imaging findings.
F = female; M = male; y = yes; n = no; m = months; S = surgery; XRT = radiation; C = chemotherapy; Unk = unknown; (–) = negative; (+) = positive; MIB-1 = methylation-inhibited binding protein 1; PTEN = phosphage and tensin; NE = nonevaluable.

demonstrating predominantly trace to <50% restriction. Three de novo lesions demonstrated extracranial extension, one into the skull, one into the adjacent scalp tissues, and the third through the skull base and into the masticator space (Fig 2, Table 3). There were no reported distant metastases.

Clinical Characteristics

The majority of subjects (10 of 25) presented with headaches. Traumatic fall related to hemiparesis/hemiplegia was also a common presentation (5 of 25). A small number of subjects also presented with seizure or loss of consciousness (2 of 25). Progressive speech changes and cognitive decline were noted in 3 of 25 subjects. In 5 subjects, presenting symptoms were not available.

Treatment records were available in 20 of 25 subjects. The majority of subjects (13) underwent maximal safe resection and concurrent chemotherapy and radiation with temozolamide. Three subjects underwent surgery alone, and 4 had a combination of radiation and surgical therapy without systemic chemotherapy.

Survival data were obtained on 16 of 25 subjects, with 9 subjects lost to follow up because of transfer out of our hospital system, or hospice care. The overall survival ranged from .5 to 66 months, with an overall 11.8 month survival including both de novo and treatment-induced subjects. In subjects with de novo GSC, survival was an average of 13.5 months, and 4.7 months in treatment-induced GSC. Survival in those subjects who received a combination of surgery, radiation, and chemotherapy was longest, averaging 17.6 months. Survival decreased when only surgery and radiation therapy were used for treatment (11.8 months), with even further decrease in subjects who received surgery alone (6.7 months) (Table 2).

Statistical Analysis

Logistic regression analyses demonstrated no significant correlation between molecular markers with original lesion size (coefficient = –.0785, P= .8,807 for p53; coefficient = –.2,181, P = .6,237 for PTEN; coefficient = –.2,728, P = .633 for MGMT), survival (coefficient = –.055, P = .76 for p53; coefficient = .066, P = .68 for PTEN; coefficient = –.17, P = .27 for MGMT), lesion composition (coefficient = .211, P = .781 for p53; coefficient = 1.12, P = .095 for PTEN; coefficient = .088, P= .92 for MGMT), nodularity (coefficient = –19.11, P = .2 for p53; coefficient = –.134, P = .92 for PTEN; coefficient = –1.1, P = .5 for MGMT), extracranial extension (coefficient = 17.99, P = .31 for p53; coefficient = –.9, P = .55 for PTEN; coefficient = –17.8, P = .45 for MGMT), and enhancement characteristics (coefficient = –.96, P= .27 for p53; coefficient = .81, P= .3 for PTEN; coefficient = –.31, P = .78 for MGMT). The PTEN marker correlation with lesion composition was closest to significance.

Correlation was performed between overall survival and sarcomatous tissue percentage within the tumors in the 15 patients who had this information available. There was no significant correlation between these variables (coefficient = .0408, P= .89).

Discussion

GSC is a rare primary high-grade primary brain neoplasm which characteristically abuts a dural surface and can demonstrate both extracranial extension and extracranial

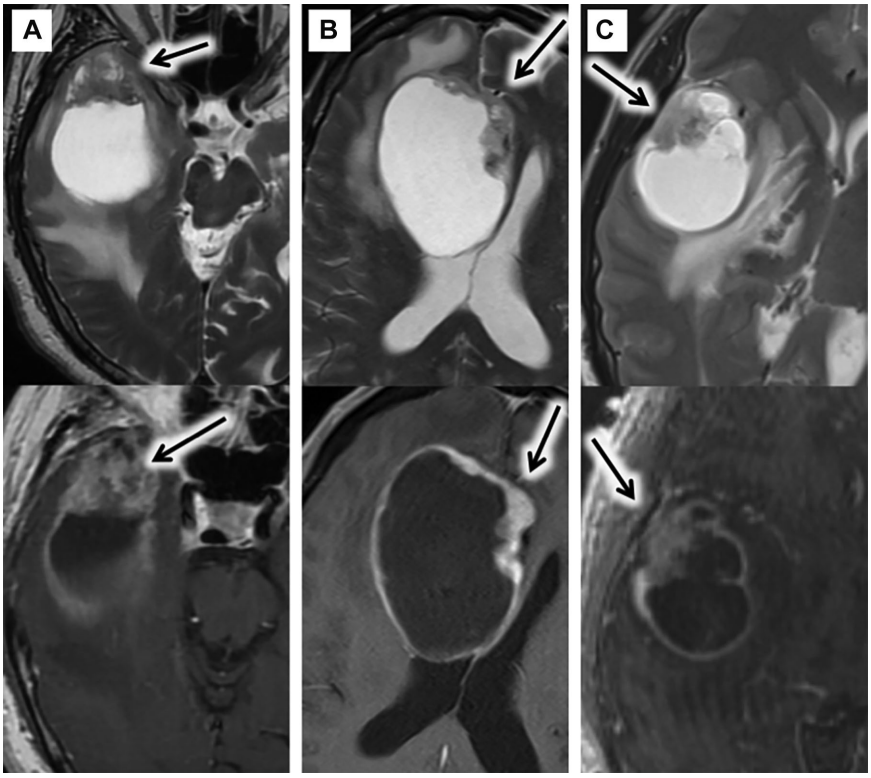

Fig 1. T2 Fast Spin Echo images acquired on 1.5T (top row) of 3 patients (A-C) with predominantly necrotic gliosarcoma masses demonstrating nodular, mass-like thickening at the site of the lesion's dural attachment (arrows) with corresponding enhancement of the nodular, mass-like thickening as seen on T1 postcontrast images acquired on 1.5T (bottom row, arrows).

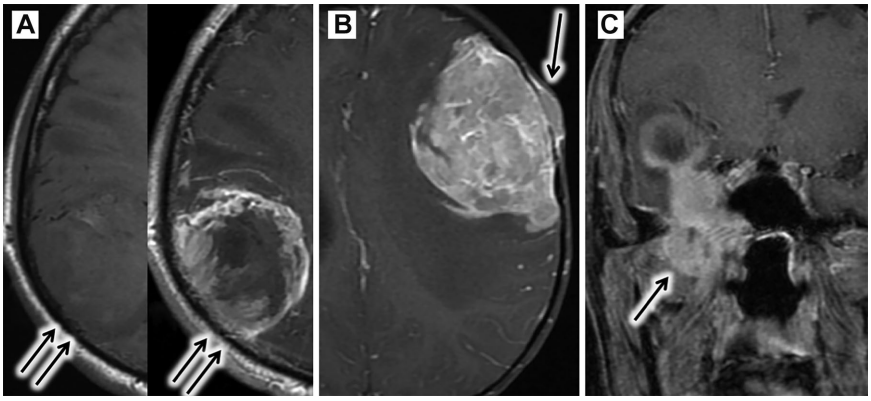

Fig 2. Three patients demonstrating gradations of extracranial involvement of gliosarcoma. Early skull invasion (A, precontrast T1 Spin Echo (SE) acquired on 1.5T on the left, and postcontrast T1 SE acquired on 1.5T on the right) with subtle calvarial erosions (arrows), skull and scalp invasion seen on postcontrast T1 SE acquired on 1.5T (B, arrow), and frank invasion of the skull base into the masticator space seen on postcontrast T1 SE acquired on 1.5T (C, arrow) are demonstrated. Interestingly, the subject in B was only 5 years old at the time of presentation, a rarity for this lesion which usually presents in the adult population.

metastases.[10,13–15] Both imaging findings and genetic findings overlap with GBM. While separate imaging and histologic case series have been performed, a large series correlating these findings has never been reported. In this study correlating immunohistochemical and imaging findings in 25 patients, we found no significant correlation between imaging characteristics and individual molecular markers; however, we did find all lesions to be IDH(–), and we also noted imaging trends in these lesions.

Histologically, GSC is composed of both mesenchymal and glial components. Though they have a biphasic histologic pattern, both of these components are found to be similar for genetic markers, suggesting that these lesions are in fact monoclonal (Fig 3).[16,17]

Interestingly, in one study of 11 patients, the histologic composition of this lesion appeared to affect prognosis, with lesions demonstrating a higher percentage of sarcomatous components showing slightly improved survival time in comparison to lesions which were predominantly glial.[18] This concept was reinforced in an additional study of 16 patients, demonstrating that lesions that had more meningiomatous elements conferred improved survival time.[7] In our study, we found no significant correlation between these variables; however, our evaluation

Table 3. Imaging Characteristics of GSC

Case	Location	Size (cm)	T2	T1	T1+C	GRE	DWI	Composition	Dural Contact	EC Extension
1	L temporal	6.6	Hyper	Hypo	Peripheral	–	–	Necrotic	– (ependymal)	–
2	R frontoparietal	6.3	Mixed	Mixed	Mixed	<50%	<50%	Solid	+	+ (skull)
3	R frontal	5.4	Mixed	Mixed	Peripheral	<50%	<50%	Mixed	+	–
4	R temporal	4.8	Hyper	Hypo	Peripheral	<50%	–	Necrotic	+	–
5	R temporal	7.2	Hyper	Hypo	Peripheral	>50%	–	Necrotic	+	–
6	R temporal	7	Hyper	Hypo	Peripheral	<50%	–	Necrotic	+	+ (masticator space)
7	R frontal	5.9	Hyper	Hypo	Peripheral	<50%	–	Necrotic	+	–
8	R temporal	7	Mixed	Mixed	Mixed	>50%	<50%	Necrotic	+	–
9	L temporal	6	Mixed	Hypo	Mixed	–	–	Mixed	+	–
10	R temporal	3.8	Mixed	Hypo	Peripheral	–	>50%	Solid	– (pial)	–
11	R frontal	7	Hyper	Hypo	Peripheral	<50%	–	Necrotic	+	–
12	R frontal	3.5	Mixed	Hypo	Mixed	>50%	Trace	Solid	– (ependymal)	–
13	R temporal	4.3	Mixed	Hypo	Mixed	–	–	Mixed	+	–
14	R temporal	2.3	Hyper	Hypo	Peripheral	<50%	–	Necrotic	+	–
15	L frontoparietal	4.5	Hypo	Mixed	Diffuse	Trace	>50%	Solid	+	–
16	R frontotemporal	4.6	Mixed	Hypo	Diffuse	<50%	<50%	Solid	+	–
17	R parietooccipital	3.9	Mixed	Hypo	Diffuse	<50%	<50%	Solid	+	–
18	L occiptal	7.5	Mixed	Hypo	Mixed	>50%	>50%	Solid	– (ependymal)	–
19	L frontal	7.6	Hypo	Mixed	Diffuse	Trace	<50%	Solid	+	+ (scalp)
20	R frontotemporal	5.7	Mixed	Hypo	Mixed	Trace	–	Solid	+	–
21	L frontal	6	Hypo	Hypo	Mixed	Unk	–	Solid	+	–
22	R temporal	7.2	Hypo	Hypo	Peripheral	–	<50%	Necrotic	+	–
23	L temporal	6.3	Mixed	Hypo	Mixed	Unk	>50%	Mixed	+	–
24	L temporal	3.5	Hypo	Mixed	Diffuse	Unk	>50%	Solid	+	–
25	R temporal	6.2	Unk	Dark	Mixed	Unk	Unk	Solid	+	–

All subjects with corresponding imaging findings.
R = right; L = left; cm = centimeters; Hyper = hyperintense to gray matter; Hypo = hypointense to gray matter; (–) = negative; (+) = positive; GRE = gradient echo; DWI = diffusion weighted imaging; EC = extracranial.

was limited to only 15 patients who had both survival time and evaluable histopathology, and by differences in the amount of resected tissue in each case which likely resulted in a component of sampling error.

Genetic information on GSC remains scant, preventing unambiguous classification of this tumor. Up to this point, EGFR amplification and TP53 mutations have been found to be rare in GSC; however, PTEN mutation and $p16^{INK4a}$ have been found to be more common (37-45%).[5,17,19] Our study findings slightly differed with these data, demonstrating p53 positivity in the majority of lesions (14 of 16) using a 30% cutoff, and PTEN positivity in 9 of 14 lesions. There was no EGFR amplification in the 17 tumors tested. MGMT methylation is also very rare in GSC, as we also noted in our series with only two lesions demonstrating methylation.[8] In keeping with the majority of other series, all tumors in our study were negative for the IDH-R132 mutation, supporting the concept that GSC is almost universally wild-type with only rare exceptions.[5,8] In one interesting case from our series, a GSC arose in the resection cavity of a IDH wild-type grade 2 diffuse fibrillary astrocytoma––a lesion often found to be IDH1-mutated.[20] Overall, in our study, we found no significant correlation between molecular markers and lesion imaging characteristics or survival time. However, analyses are limited in this population size and larger studies may delineate a relationship between lesion molecular characteristics and imaging findings.

Unlike secondary GBM, GSC is thought to rapidly arise without a less malignant precursor lesion.[17] Imaging in the majority of our cases supported this, with most patients presenting with de novo lesions having no history of a precursor lesion. However, one of our cases demonstrated features which appeared to contradict the accepted rapid onset timeline. In one subject with a history of neurofibromatosis type-1, a small enhancing lesion deep to the cortex without dural contact was noted on a routine scan. This was clinically thought to be a neurofibromatosis-1-related lesion but not biopsy proven. The patient was lost to follow up for 12 years, but when subsequently presented with headaches, had imaging demonstrating marked growth of the lesion which now directly contacted the dural surface (Fig 4) and was biopsy-proven GSC. This suggests that some of these lesions may remain dormant for a longer period of time than previously thought. Though this represents only a single case, findings also posit a parenchymal origin of this lesion with subsequent extension to the dura.

Another unique feature of GSC is its ability to metastasize to multiple sites outside of the CNS.[14,21] Multiple rare primary locations for these lesions have been described, including the cerebellum, pineal region, cerebellopontine angle, intraventricular, and within the spinal cord.[11,22–26] While distant metastases were not reported in this group of patients, extracranial local extension was seen in three cases, with one involving the masticator space. The more commonly seen finding of temporal lobe involvement was noted in the majority of our studies, concordant with a study of 353 GSC through the Surveillance, Epidemiology, and End Results (SEER) database which demonstrated that GSC had a higher propensity for temporal lobe involvement than GBM.[27]

Multiple studies have shown that the general imaging appearance of GSC is indistinguishable from GBM and the WHO considers it an uncommon variant. An exception is noted in cases where extracranial tumor extension is seen.[15,28,29] Though findings of a centrally necrotic lesion with irregular

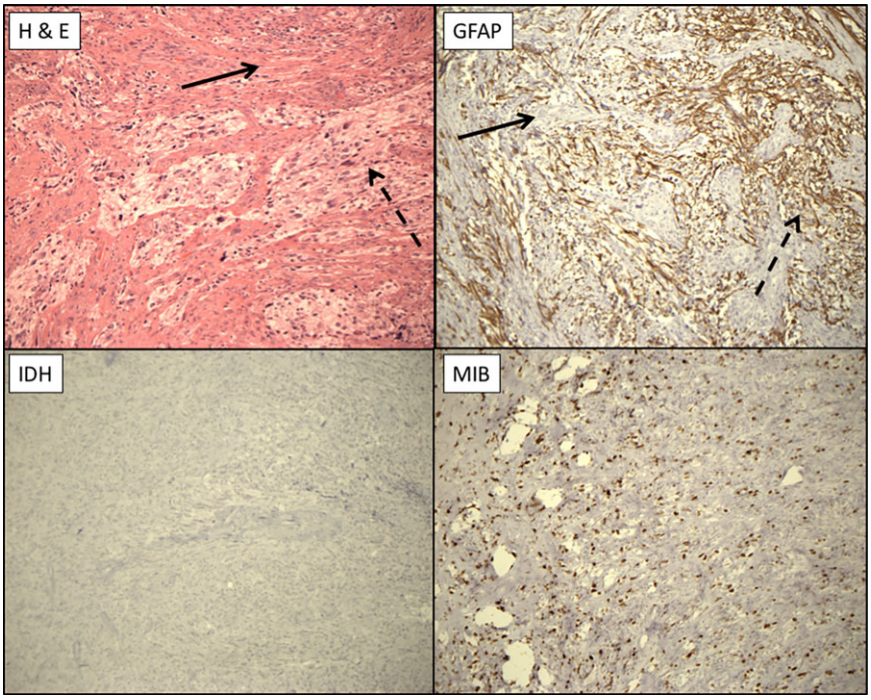

Fig 3. H&E: This gliosarcoma (GSC) contains intermingled spindled mesenchymal elements (solid arrow) surrounded by nests of glial elements (dashed arrow) (hematoxylin and eosin × 100). GFAP: The glial elements are positive in this glial fibrillary acidic protein (GFAP) immunostain (dashed arrow), whereas the spindled mesenchymal elements are negative (solid arrow) (GFAP x 100). IDH-1: This gliosarcoma is negative for isocitrate dehydrogenase 1 (IDH-1) R132 clone immunostaining, indicating a lack of mutated IDH (IDH-1 × 100). MIB-1: Methylation-inhibited binding protein 1(MIB-1) immunostain was greater than 20% in all GSC specimens (MIB-1 × 100).

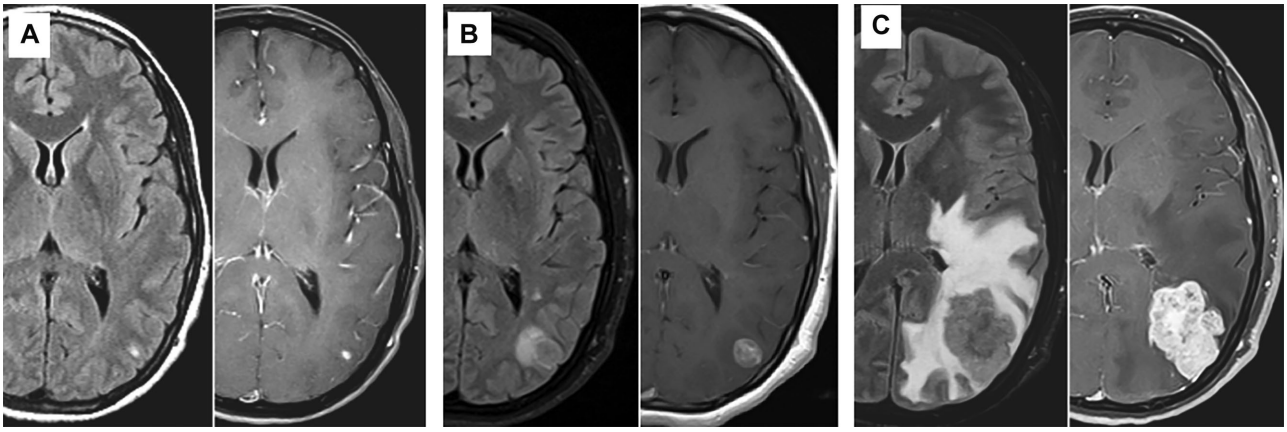

Fig 4. Composite fluid attenuation inversion recovery (left) and T1 SE postcontrast (right) images all acquired on 1.5T demonstrate a small subcortical enhancing lesion in the left parietal lobe (A) which subsequently grew in size and was found to contact the dura in a scan obtained 12 years later (B) with significant growth in the next 6 months (C). This lesion was histologically confirmed to be gliosarcoma.

rim-enhancement and aggressive features cannot be differentiated from GBM by imaging alone, our study did support a pattern of two imaging subgroups: predominantly necrotic lesions demonstrating nodular mass-like thickening at the site of dural attachment, and predominantly solid lesions. We propose that in cases where imaging demonstrates a necrotic dural-based lesion with nodular, mass-like thickening at the site of dural attachment, the rare GSC variant should be considered.

Prognosis for GSC is poor, with a study of 353 patients reporting a median survival time of 9 months.[26] Though GSC has a larger rate of gross-total resection than GBM due to its margins being more well defined, overall survival time was not significantly different in a large analysis of the National Cancer Database, or in other case series.[27,30,31] In patients receiving a combination of surgery, chemotherapy, and radiation therapy, survival time improved to 12.9 months from 5.5 months in patients without this combination. A trend of improved survival was also seen with MGMT promoter methylation.[30] Both extent of resection and adjuvant chemotherapy were noted to be independent prognostic factors for increased survival in elderly GSC patients.[32] A multimodality approach has been found to be overall associated with improved outcomes.[33] This was also found to be true in our study where subjects receiving a combination of surgical, radiation, and chemotherapies demonstrated the longest survival, and therapy with surgery and radiation conferred shorter survival times, with the shortest

noted in subjects who received surgery alone. This further demonstrates the importance of multiomodality therapy in treatment of this rare and highly malignant lesion.

GSC was IDH(–) in all cases, supporting the current understanding of this lesion being a wild-type GBM variant. Additional molecular markers demonstrated no significant correlation with imaging findings in this cohort which is the largest to date containing both imaging and histopathologic/molecular findings.

References

1. Delfanti RL, Piccioni DE, Handwerker J, et al. Imaging correlates for the 2016 update on WHO classification of grade II/III gliomas: implications for IDH, 1p/19q and ATRX status. J Neurooncol 2017;135:601-9.
2. Koh J, Cho H, Kim H, et al. IDH2 mutation in gliomas including novel mutation. Neuropathology 2015;35:236-44.
3. Wesseling P, Capper D. WHO 2016 Classification of gliomas. Neuropathol Appl Neurobiol 2017;44:139-50.
4. Chen N, Yu T, Gong J, et al. IDH1/2 gene hotspot mutations in central nervous system tumours: analysis of 922 Chinese patients. Pathology 2016;48:675-83.
5. Oh JE, Ohta T, Nonoguchi N, et al. Genetic alterations in gliosarcoma and giant cell glioblastoma. Brain Pathol 2016;26:517-22.
6. Louis DN, Ohgaki H, Wiestler OD, et al. The 2007 WHO classification of tumours of the central nervous system. Acta Neuropathol 2007;114:97-109.
7. Singh G, Das KK, Sharma P, et al. Cerebral gliosarcoma: analysis of 16 patients and review of literature. Asian J Neurosurg 2015;10:195-202.
8. Lee D, Kang SY, Suh YL, et al. Clinicopathologic and genomic features of gliosarcomas. J Neurooncol 2012;107:643-50.
9. Zhang BY, Chen H, Geng DY, et al. Computed tomography and magnetic resonance features of gliosarcoma: a study of 54 cases. J Comput Assist Tomogr 2011;35:667-73.
10. Dwyer KW, Naul LG, Hise JH. Gliosarcoma. MR features. J Comput Assist Tomogr 1996;20:719-23.
11. Han L, Zhang X, Qiu S, et al. Magnetic resonance imaging of primary cerebral gliosarcoma: a report of 15 cases. Acta Radiol 2008;49:1058-67.
12. Romero-Rojas AE, Diaz-Perez JA, Ariza-Serrano LM, et al. Primary gliosarcoma of the brain: radiologic and histopathologic features. Neuroradiol J 2013;26:639-48.
13. Sampaio L, Linhares P, Fonseca J. Detailed magnetic resonance imaging features of a case series of primary gliosarcoma. Neuroradiol J 2017;30:546-53.
14. Choi TM, Cheon YJ, Jung TY, et al. A stable secondary gliosarcoma with extensive systemic metastases: a case report. Brain Tumor Res Treat 2016;4:133-7.
15. Nguyen QD, Perry A, Graffeo CS, et al. Gliosarcoma with primary skull base invasion. Case Rep Radiol 2016;2016:1762195.
16. Biernat W, Aguzzi A, Sure U, et al. Identical mutations of the p53 tumor suppressor gene in the gliomatous and the sarcomatous components of gliosarcomas suggest a common origin from glial cells. J Neuropathol Exp Neurol 1995;54:651-6.
17. Reis RM, Konu-Leblebicioglu D, Lopes JM, et al. Genetic profile of gliosarcomas. Am J Pathol 2000;156:425-32.
18. Salvati M, Caroli E, Raco A, et al. Gliosarcomas: analysis of 11 cases do two subtypes exist? J Neurooncol 2005;74:59-63.
19. Actor B, Cobbers JM, Buschges R, et al. Comprehensive analysis of genomic alterations in gliosarcoma and its two tissue components. Genes Chromosomes Cancer 2002;34:416-27.
20. Rajeswarie RT, Rao S, Nandeesh BN, et al. A simple algorithmic approach using histology and immunohistochemistry for the current classification of adult diffuse glioma in a resource-limited set-up. J Clin Pathol 2018;4:323-9.
21. Chen L, Xiao H, Xu L, et al. A case study of a patient with gliosarcoma with an extended survival and spinal cord metastases. Cell Biochem Biophys 2012;62:391-5.
22. Doddamani RS, Meena RK, Selvam MM, et al. Intraventricular gliosarcomas: literature review and a case description. World Neurosurg 2016;90:707-12.
23. Kumar RM, Finn M. Primary multifocal gliosarcoma of the spinal cord. Rare Tumors 2016;8:6102.
24. Sugita Y, Terasaki M, Tanigawa K, et al. Gliosarcomas arising from the pineal gland region: uncommon localization and rare tumors. Neuropathology 2016;36:56-63.
25. Duan H, Kitazawa K, Yako T, et al. Gliosarcoma in the cerebellopontine angle with rapid tumor growth and intratumoral hemorrhage. World Neurosurg 2016;92:517-21.
26. Moon SK, Kim EJ, Choi WS, et al. Gliosarcoma of the cerebellar hemisphere: a case report and review of the literature. Korean J Radiol 2010;11:566-70.
27. Kozak KR, Mahadevan A, Moody JS. Adult gliosarcoma: epidemiology, natural history, and factors associated with outcome. Neuro Oncol 2009;11:183-91.
28. Mason A, Villavicencio AT, Nelson EL, et al. Post-treatment gliosarcoma extension into the pterygomaxillary fossa: literature review and case report. Cureus 2016;8:700.
29. Sade B, Prayson RA, Lee JH. Gliosarcoma with infratemporal fossa extension. Case report. J Neurosurg 2006;105:904-7.
30. Frandsen J, Orton A, Jensen R, et al. Patterns of care and outcomes in gliosarcoma: an analysis of the national cancer database. J Neurosurg 2017:1–6.
31. Kumar P, Singh S, Kumar P, et al. Gliosarcoma: an audit from a single institution in India of 24 post-irradiated cases over 15 years. J Cancer Res Ther 2008;4:164-8.
32. Shin JY, Yoon JK, Diaz AZ. Gliosarcoma in septuagenarians and octogenarians: what is the impact of adjuvant chemoradiation? J Clin Neurosci 2017;45:77-82.
33. Jain A, Correia J, Schweder P, et al. Analysis of outcomes of multidisciplinary management of gliosarcoma: a single-center study, 2000–2013. World Neurosurg 2017;106:30-6.